Redox-sensitive stimulation of type-1 ryanodine receptors by the scorpion toxin maurocalcine.

Michel Ronjat, José Pablo Finkelstein, Paola Llanos, Luis Montecinos, Hicham Bichraoui, Michel de Waard, Cecilia Hidalgo, Ricardo Bull

REDOX-SENSITIVE STIMULATION OF TYPE-1 RYANODINE RECEPTORS BY THE SCORPION TOXIN MAUROCALCINE

Michel Ronjat[a,b,c], José Pablo Finkelstein[d,e], Paola Llanos[d], Luis Montecinos[d,e], Hicham Bichraoui[a,b], Michel De Waard[a,b,c], Cecilia Hidalgo[d,e], Ricardo Bull[d,e].

[a]Unité Inserm 836, Grenoble Institute of Neuroscience, Site Santé, BP 170, 38042 Grenoble, [b]Université Joseph Fourier, Grenoble, France; [c]Lab. Ex ICST, [d]Centro de Estudios Moleculares de la Célula; [e]Programa de Fisiología y Biofísica, Instituto de Ciencias Biomédicas, Facultad de Medicina, Universidad de Chile, Independencia 1027, Santiago 7, Chile.

Corresponding author: Dr. Ricardo Bull, Programa de Fisiología y Biofísica, ICBM, Facultad de Medicina, Universidad de Chile, Independencia 1027, Santiago 7, Chile. Postal Code: 838-0453.
Phone: (56-2) 2978-6313; FAX: (56-2) 2777-6916.
E-mail: rbull@med.uchile.cl

Co-corresponding author: Dr. Michel Ronjat, Unité Inserm 836, Grenoble Institute of Neuroscience, Site Santé, BP 170, 38042, Grenoble, France.
Phone: 33-(0)4 56 52 05 65; FAX: 33-(0)4 56 52 05 72.
E-mail: michel.ronjat@ujf-grenoble.fr

Running title: Redox-sensitive RyR stimulation by Maurocalcine

Keywords: Ca^{2+} release; sulfhydryl oxidation; ryanodine binding; planar lipid bilayers; Mg^{2+} inhibition; channel sub-conductance.

ABSTRACT

The scorpion toxin maurocalcine acts as a high affinity agonist of the ryanodine receptor isoform expressed in skeletal muscle. Here, we investigated the effects of the reducing agent dithiothreitol or the oxidizing reagent thimerosal on type-1 ryanodine receptor stimulation by maurocalcine. Pre-incubation of skeletal sarcoplasmic reticulum vesicles with dithiothreitol did not affect maurocalcine-induced Ca^{2+} release compared to native vesicles, but thimerosal prevented this response. Maurocalcine enhanced more effectively equilibrium [^{3}H]-ryanodine binding to dithiothreitol-treated than to native reticulum vesicles, and increased 5-fold the apparent K_i for Mg^{2+} inhibition of [^{3}H]-ryanodine binding to native vesicles. Single calcium release channels incorporated in planar lipid bilayers displayed a long-lived open sub-conductance state after maurocalcine addition. The fractional time spent in this sub-conductance state decreased when lowering the cytoplasmic Ca^{2+} concentration from 10 μM to 0.1 μM or at cytoplasmic Mg^{2+} concentrations ≥ 30 μM. At 0.1 μM Ca^{2+} concentration, only channels that displayed poor activation by Ca^{2+} were readily activated by 5 nM maurocalcine; subsequent incubation with thimerosal abolished the sub-conductance state induced by maurocalcine. We interpret these results as an indication that maurocalcine acts as a more effective type-1 ryanodine receptor channel agonist under reducing conditions.

1. INTRODUCTION

Ryanodine receptors (RyR) are intracellular Ca^{2+} release channels with a key role in skeletal muscle excitation-contraction coupling [1]. Physiological activation of type-1 RyR (RyR1) channels, the prevalent isoform expressed in adult mammalian skeletal muscle, occurs as a consequence of conformational changes of the interacting dihydropyridine receptors (DHPR) induced by membrane depolarization [2]. Several cellular components and covalent modifications of the protein modify RyR1 activity, including ATP, cyclic ADP ribose, H^+ and Mg^{2+}, phosphorylation or changes in RyR1 redox state [1]. In particular, RyR redox state markedly influences the effects of physiological RyR agonists or inhibitors, such as Ca^{2+}, Mg^{2+} and ATP, on RyR activity [3, 4]. Skeletal RyR1 channels possess a few cysteine residues with high reactivity to redox agents at physiological pH [5, 6]. Modification of essential sulfhydryl residues involved in the gating of RyR1 channels modulates the apparent Ca^{2+} affinity of both, the activating high affinity and the inhibitory low affinity Ca^{2+}/Mg^{2+} binding sites [7-9]. Oxidizing agents decrease significantly the inhibitory effects of Mg^{2+} on RyR1 activity [10, 11].

Under conditions of sustained or strenuous exercise, skeletal muscle cells increase the production of reactive oxygen species that may affect RyR1 activity *in vivo* [12]. Consequently, to explore if the redox changes that occur in skeletal muscle during exercise-associated contractile activity modify RyR1-mediated Ca^{2+} release, it becomes important to study RyR1 channels under different redox conditions, which affect in particular their Ca^{2+} activation/Mg^{2+} inhibition profiles and the effects of selective agonists. Cell permeable compounds that bind with high-affinity to RyR channels and modify their function are

useful tools to study RyR1 function in a cellular context. The scorpion toxin maurocalcine (MCa), a 33-mer basic peptide cross-linked by three disulfide bridges that crosses cell membranes within 1-2 min [13, 14] is a high-affinity and reversible RyR1 agonist. Addition of MCa at nanomolar concentrations to RyR1 channels incorporated in planar lipid bilayers induces a well-defined channel sub-conductance state, with long-lasting openings to a level equivalent to 50-60% of maximal current [15]. Maurocalcine also activates channels modified with ryanodine or lacking the FK506-binding protein [16, 17]. At 10 µM free Ca^{2+} concentration ($[Ca^{2+}]$), MCa concentrations in the nM range (EC_{50}=12 nM) stimulate [^{3}H]-ryanodine binding to RyR1 [16]. Maurocalcine shifts the stimulation of [^{3}H]-ryanodine binding by Ca^{2+} to lower concentrations and decreases the inhibitory effects of high $[Ca^{2+}]$ [17]. These findings correlate well with the marked stimulation of Ca^{2+} release induced by MCa addition to skeletal SR vesicles (EC_{50}=17.5 nM) or cultured myotubes [17].

In this work, we used isolated skeletal SR vesicles enriched in triads to test the effects of MCa on RyR1-mediated Ca^{2+} release and [^{3}H]-ryanodine binding, under the different redox conditions produced by the reducing agent dithiothreitol (DTT) or the oxidizing agent thimerosal. We also tested the effects of DTT, thimerosal and of varying free Mg^{2+} concentrations ($[Mg^{2+}]$) on the sub-conductance state induced by MCa in single RyR1 channels incorporated in planar lipid bilayers. Our results strongly suggest that, under reducing conditions, MCa is an effective high-affinity RyR1 channel agonist. In addition, we show that incubation with thimerosal hinders RyR1 channel activation by MCa at resting Ca^{2+} concentration.

2. MATERIALS AND METHODS

2.1 Materials

All reagents used were of analytical grade. Lipids were from Avanti Polar Lipids, Inc. (Birmingham, AL). Bovine serum albumin, DTT, ryanodine, thimerosal, and protease inhibitors (leupeptin, pepstatin A, benzamidine, trypsin inhibitor, phenylmethylsulfonyl fluoride) were from Sigma Chemical Co. (St. Louis, MO). Calcium Green-2 was from Molecular Probes, Inc (Eugene, OR) and [^{3}H]-ryanodine from NEN Life Sciences (Boston, MA). Maurocalcine was synthesized as described [15].

2.2 Membrane preparations

SR vesicles were isolated from fast skeletal muscle of New Zealand rabbits as described [18]. Aliquots of vesicle-containing suspensions frozen in liquid nitrogen were stored at -80ºC for up to 30 days. The Bioethics Committee for Investigation in Animals of the Facultad de Medicina, Universidad de Chile approved all experimental protocols used in this work.

2.3 Calcium release experiments

Ca^{2+} release was determined in a fluorescence spectrometer, using the fluorescent probe Calcium Green-2 to detect extravesicular Ca^{2+} concentration changes. To this end,

triad-enriched SR vesicles were diluted to 0.2 mg per ml in a solution containing (in mM): 100 KCl, 10 phosphocreatine plus 15 IU/ml creatine phosphokinase, 20 MOPS/Tris pH 7.2 and 0.09 μM Calcium Green-2. After addition of SR vesicles, the [Ca^{2+}] of the above medium (Mg^{2+}-free) was determined with a Ca^{2+} electrode (Orion, Beverly, MA) calibrated with a commercial kit (WPI, Sarasota, FL). Ca^{2+} uptake was initiated at 25°C by simultaneous addition of 2.0 mM $MgCl_2$ plus 2.0 mM ATP ([Mg^{2+}] = 0.35 mM). Ca^{2+} release was induced by addition of MCa, or caffeine. Assuming a K_d of 0.4 μM, the [Ca^{2+}] was calculated from Calcium Green-2 fluorescence (F) according to the equation:

$$[Ca^{2+}] = K_d (F_{max}-F)/(F-F_{min})$$

The maximal (F_{max}) and the minimal (F_{min}) values of fluorescence were determined after addition of 1.0 mM $CaCl_2$ or 10 mM ethyleneglycol-bis(ß-aminoethyl ether) N, N, N', N'-tetraacetic acid (EGTA), respectively. In Mg^{2+}-free solutions the values of [Ca^{2+}] calculated according to the above equation from determinations of Calcium Green-2 fluorescence, coincided with the [Ca^{2+}] values determined with the Ca^{2+} electrode. Caffeine addition produced some quenching of Calcium Green-2 fluorescence (10% at 5 mM caffeine), which was corrected to calculate extravesicular [Ca^{2+}] levels.

2.4 Equilibrium [^{3}H]-ryanodine binding

SR vesicles (1 mg/ml) were incubated at 37°C for 2 h in a solution containing (in mM): 150 KCl, 20 MOPS-Tris, pH 7.2, 1 EGTA, 1 $CaCl_2$, 10 nM [^{3}H]-ryanodine, plus/minus MCa at the concentrations indicated in the text. In some experiments, vesicles were pre-incubated for 15 to 30 min with DTT (0.5 or 1 mM). Non-specific binding was

determined by addition of 10 µM ryanodine to the above incubation solution. After incubation, [^{3}H]-ryanodine binding was determined by filtration as described [19].

2.5 Single channel experiments

Channel recordings were obtained as reported [20-22]. The *cis* (cytoplasmic) solution contained 0.5 mM Ca^{2+}-HEPES and 225 mM HEPES-Tris, pH 7.4. To set the desired [Ca^{2+}] and/or [Mg^{2+}], N-(2-hydroxyethyl)-ethylenediamine-triacetic acid (HEDTA) and/or EGTA were added to the cis compartment. Total concentrations of HEDTA, EGTA, Ca^{2+} and Mg^{2+} required for each [Ca^{2+}] and/or [Mg^{2+}] were calculated with the WinMAXC program (www.stanford.edu/~cpatton). The *trans* (luminal) solution contained 40 mM Ca^{2+}-HEPES, 15 mM Tris-HEPES, pH 7.4; therefore, in all experiments the charge carrier was Ca^{2+}. The lipid bilayer was held at 0 mV; channel recordings were obtained at 22 ± 2°C. Current data were filtered at 400 Hz (-3 dB) using an eight-pole low-pass Bessel type filter (902 LPF, Frequency Devices Inc., Haverhill, MA). Data were digitized at 2 kHz with a 12-bit A/D converter (Labmaster DMA interface, Scientific Solutions, Inc., Solon, OH) using the commercial software Axotape (Molecular Devices Corporation, Sunnyvale, CA).

We defined P_o as the fraction of time a single RyR1 channel spent in the open state in the absence of MCa. Addition of MCa induced a well-defined sub-conductance state; we defined P_{MCa} as the fractional time the channel spent in this sub-conductance state, and P_{oB} as the fractional time a channel not dwelling in the MCa-induced sub-conductance state spent in the open state (see Fig. S1). Fractional times were computed with the pClamp

commercial software (Molecular Devices Corporation, Sunnyvale, CA). Nonlinear fitting of data was performed using the SigmaPlot software (Systat Software Inc., Richmond, CA).

2.6 Data expression and statistical analysis

Data are expressed as Mean ± Standard Error (SE). Student's *t*-test was used for statistical analysis, unless specified otherwise.

3. RESULTS

3.1 Effects of maurocalcine and caffeine on vesicular Ca^{2+} release

Active Ca^{2+} uptake, mediated by the sarcoplasmic/endoplasmic reticulum Ca^{2+}-ATPase (SERCA), was started by adding Mg-ATP to triad-enriched SR vesicles isolated from rabbit fast skeletal muscle. Addition of Mg-ATP to native SR vesicles produced a fast decrease in extravesicular [Ca^{2+}] (Fig. 1A), which decreased on average from 23.8 ± 5.9 µM (N = 7, measured with a calcium electrode) to < 0.15 µM, calculated from the decrease in probe fluorescence. Addition of MCa to native SR vesicles actively loaded with calcium induced fast Ca^{2+} release, as illustrated in the fluorescence record from the representative experiment shown in Figure 1A. To favor the reduced state of RyR1, SR vesicles were pre-incubated with the reducing agent DTT before initiating Ca^{2+} uptake. Addition of MCa effectively promoted Ca^{2+} release from calcium-loaded SR vesicles pre-incubated with DTT, as evidenced by the rapid increase in probe fluorescence (Fig. 1B). The release of

Ca^{2+} from native or DTT-treated vesicles was transient, indicating both that RyR1 channels closed/inactivated rapidly after activation with MCa and that pre-incubation with DTT did not modify SERCA activity. Similar behaviors were observed in four independent experiments carried out with native or DTT-treated vesicles. To test the effects of RyR1 oxidation, we added thimerosal (10 µM) after Ca^{2+} uptake completion. In contrast to the behavior displayed by native or DTT-treated vesicles, subsequent addition of MCa (200 nM) did not stimulate release, whereas further addition of caffeine effectively induced transient Ca^{2+} release (Fig. 1C), showing that thimerosal did not inhibit RyR1 or SERCA function. This same behavior was observed in five independent experiments. Addition of a higher concentration of MCa (400 nM) did not induce Ca^{2+} release from thimerosal-treated vesicles (not shown), suggesting that - at the low [Ca^{2+}] present in the extravesicular solution after Ca^{2+} uptake - oxidized RyR1 channels have significantly decreased MCa affinity compared to native or reduced channels.

The results illustrated in Figure 1 show that the reducing agent DTT did not hinder MCa-induced Ca^{2+} release through RyR1 channels while incubation with the SH-oxidizing agent thimerosal prevented MCa-induced but not caffeine-induced Ca^{2+} release. Thus, redox agents have opposite effects on Ca^{2+} release induced by MCa or caffeine, since caffeine is a more effective agonist of RyR1-mediated Ca^{2+} release under oxidizing than under reducing conditions (Beltrán et al, manuscript in preparation). To test the hypothesis that redox agents modify the effectiveness of MCa as RyR1 agonist, we measured under different redox conditions the effects of MCa on vesicular [^{3}H]-ryanodine binding and on the activity of single RyR1 channels incorporated into planar lipid bilayers.

3.2 Maurocalcine increases equilibrium [^{3}H]-ryanodine binding. Effects of DTT and Mg^{2+}

The plant alkaloid ryanodine is a highly selective reagent, considered the gold standard to monitor RyR channel function. A good correlation between single RyR1 channel activity and [^{3}H]-ryanodine binding density to skeletal SR vesicles has been reported [23, 24]. Maurocalcine stimulated [^{3}H]-ryanodine binding density when added to native SR vesicles (Fig. 2A), which correlates with the stimulation of Ca^{2+} release described above. Native (untreated) SR vesicles incubated with MCa (50 nM) exhibited an increase of 6.3 ± 0.5 fold (Mean ± SE, N=3) in equilibrium [^{3}H]-ryanodine binding relative to the values determined in the absence of MCa. Vesicles incubated with DTT displayed a 60% reduction, on average, of [^{3}H]-ryanodine binding relative to native vesicles (Fig. 2A), confirming the inhibitory effects of reducing agents on [^{3}H]-ryanodine binding to RyR channels [3]. Addition of 50 nM MCa to DTT-treated SR vesicles, however, resulted in higher stimulation of [^{3}H]-ryanodine binding density compared with native vesicles (Fig. 2A). In DTT-treated vesicles MCa increased [^{3}H]-ryanodine binding 11.1 ± 1.4 fold (N=3) relative to vesicles incubated only with DTT, about twice the stimulation induced by MCa in native vesicles ($p = 0.048$). Therefore, DTT enhanced the effect of MCa on [^{3}H]-ryanodine binding, which could reflect an increase in apparent affinity of RyR1 for channel activation by MCa. Irreversible RyR1 inhibition induced by long exposure to thimerosal, such as that required to measure equilibrium [^{3}H]-ryanodine binding density, precluded a detailed study of the effects of MCa on thimerosal treated vesicles.

Several reports indicate that Mg^{2+} is a potent inhibitor of RyR1 activity [1]. Interestingly, oxidizing reagents decrease the inhibitory effects of Mg^{2+} on RyR1 activity [11] while reducing agents increase the Mg^{2+} inhibition of [^{3}H]-ryanodine binding to endoplasmic reticulum vesicles isolated from rat brain cortex [3]. Here, we investigated if MCa modified the inhibition of [^{3}H]-ryanodine binding to RyR1 produced by Mg^{2+}. As illustrated in Figure 2B, incubation of native skeletal SR vesicles with 200 nM MCa significantly decreased the inhibitory effects of Mg^{2+} on equilibrium [^{3}H]-ryanodine binding, which became somewhat cooperative since MCa increased n_{Hill} from 1.0 ± 0.1 to 1.4 ± 0.1 ($p = 0.047$). Native SR vesicles incubated with MCa displayed a 5-fold higher K_i value for Mg^{2+}-mediated inhibition of [^{3}H] ryanodine binding relative to the K_i value for Mg^{2+} exhibited by control vesicles ($p = 0.008$; see Fig. 2).

3.3 Effects of maurocalcine on RyR1 single channel activity

An earlier study showed that MCa induces a distinct long-lasting sub-conductance state in native RyR1 channels incorporated in planar lipid bilayers [15]. We have previously reported that single RyR1 channels display three different responses to cytoplasmic [Ca^{2+}] changes (Fig. S2), which depend on RyR channel redox state [3, 8, 22]. Incubation with reducing agents favors the appearance of channels with “low activity”, characterized by P_o values < 0.1 in the [Ca^{2+}] range 0.1-500 μM. Partial RyR oxidation of “low activity” channels usually generates the “moderate activity” response, the typical bell-shaped response to cytoplasmic calcium previously reported for native skeletal RyR1 channels [25], with maximal activity in the 10-30 μM [Ca^{2+}] range and P_o values < 0.1 at

0.1 or 500 μM [Ca^{2+}]. Further oxidation increases channel activity at low *cis* [Ca^{2+}], increases markedly P_o to values as high as 0.99 at [Ca^{2+}] > 100 μM and suppresses the inhibitory effect of 500 μM cytoplasmic [Ca^{2+}]; we call these channel behavior the "high activity" response. Here, we tested the effects of MCa on RyR1 single channels incorporated into lipid bilayers that displayed either the low or the moderate activity behavior (Fig. S2). The effects of MCa were evaluated using two parameters, i) P_{MCa} that represents the fractional time the channel spends in the MCa induced sub-conductance state and ii) P_{oB} that represents the fractional time spent in the open state in the presence of MCa, during the intervals bridging two openings at the sub-conductance level (See Fig. S1).

The low activity single RyR1 channel depicted in Figure 3A displayed at 10 μM [Ca^{2+}] a P_o value < 0.01. Addition of 5 nM MCa induced channel openings to a well-defined sub-conductance state, with P_{MCa} = 0.50 and P_{oB} = 0.01 (Fig. 3B, top trace). In the continuous presence of MCa, lowering cytoplasmic [Ca^{2+}] to 1 μM by addition of HEDTA as chelating agent decreased P_{MCa} to a value of 0.31 while P_{oB} stayed at 0.01 (Fig. 3B, center record). Further lowering cytoplasmic [Ca^{2+}] to 0.1 μM decreased P_{MCa} even more, to a value of 0.24, while P_{oB} decreased to 0.00 (Fig. 3B, lower record).

The single moderate activity RyR1 channel, illustrated in Figure 4A, displayed P_o values of 0.01 at 500 μM [Ca^{2+}] (top trace) and of 0.65 at 10 μM [Ca^{2+}] (lower trace), respectively. Addition of 5 nM MCa at 10 μM cytoplasmic [Ca^{2+}] prompted the emergence of the sub-conductance state, with P_{MCa} = 0.84 and P_{oB} = 0.71 (Fig. 4B, top trace). In the continuous presence of MCa, lowering cytoplasmic [Ca^{2+}] to 1 μM decreased P_{MCa} to a value of 0.60 and P_{oB} to 0.32 (Fig. 4B, center record). Further lowering cytoplasmic [Ca^{2+}]

to 0.1 μM decreased both P_{MCa} and P_{oB} to 0.00 (Fig. 4B, lower record). Therefore, the reduction in cytoplasmic [Ca^{2+}] in the range of 10 to 0.1 μM decreased both P_{MCa} and P_{oB}.

Average P_{MCa} and P_{oB} values obtained at different cytoplasmic [Ca^{2+}] from several single channels that spontaneously displayed either low or moderate activity are illustrated in Figure 5. At 10 μM [Ca^{2+}], addition of 5 nM MCa induced the sub-conductance state in both low and moderate activity channels, which displayed P_{MCa} values of 0.51 ± 0.10 (N=6) and 0.78 ± 0.05 (N=5), respectively. In contrast, addition of 5 nM MCa at near resting [Ca^{2+}] (0.1 μM) modified only low activity channels, which reached P_{MCa} values of 0.24 ± 0.04 (N=11) that differed significantly from the P_{MCa} values of 0.03 ± 0.03 (N=4) exhibited by moderate activity channels ($p = 0.001$). The P_o values were similar to the P_{oB} values obtained in low or moderate activity channels, respectively, suggesting that 5 nM MCa had no effect on channel activity between the sub-conductance events (Fig. 5). As expected, however, low activity channels displayed much lower P_o and P_{oB} values than moderate activity channels at 10 μM [Ca^{2+}], but not at 0.1 μM [Ca^{2+}] (see Fig. 5).

Thimerosal increases markedly the response of low activity RyR1 channels to cytoplasmic [Ca^{2+}] and sequentially promotes the moderate and the high activity responses [8]. To test if thimerosal affects the single channel response to MCa, we added thimerosal to low activity channels treated with MCa. The single channel illustrated in Figure 6 displayed at 10 μM cytoplasmic [Ca^{2+}] a P_o value < 0.01 (Fig. 6A, top trace), typical of a low activity channel. After lowering cytoplasmic [Ca^{2+}] to 0.1 μM and adding 5 nM MCa, the channel exhibited the MCa-induced sub-conductance state, with $P_{MCa} = 0.08$ and $P_{oB} = 0.01$ (Fig. 6A, lower trace). Thimerosal was added to the cytoplasmic side to a final concentration of 200 μM; after 80 s, the cytoplasmic chamber was perfused with 20 ml of

225 mM HEPES-Tris, pH 7.4. Subsequent addition of 5 nM MCa at 0.1 μM cytoplasmic [Ca^{2+}] failed to elicit the sub-conductance state observed before incubation with thimerosal, although P_{oB} reached 0.02 (Fig. 6B, lower trace). In three independent experiments carried out at cytoplasmic [Ca^{2+}] = 0.1 μM, single low activity RyR1 channels displayed average values of P_{MCa} = 0.07 ± 0.01 and P_{oB} = 0.00 ± 0.00 after addition of 5 nM MCa. Subsequent addition of thimerosal as above decreased P_{MCa} to 0.01 ± 0.01 and increased P_{oB} to 0.02 ± 0.01 (N=3). Therefore, incubation of low activity channels with thimerosal precludes RyR1 activation by 5 nM MCa at 0.1 μM cytoplasmic [Ca^{2+}], a response probably due to modification of RyR1 cysteine residues by thimerosal.

3.4 Mg^{2+} inhibits the effects of Maurocalcine on RyR1 single channel activity

In view of the fact that SR vesicles incubated with MCa displayed 5-fold higher K_i for Mg^{2+} inhibition of [^{3}H] ryanodine binding when compared to control vesicles (Fig. 2), we investigated next the joint effects of Mg^{2+} and MCa on low activity single RyR1 channels. As illustrated in Figure 7A, after addition of 5 nM MCa at 10 μM cytoplasmic [Ca^{2+}] a low activity channel displayed P_{MCa} = 0.68 and P_{oB} = 0.06 (top record). Subsequent increase of cytoplasmic [Mg^{2+}] to 30 μM, decreased P_{MCa} to 0.35 and P_{oB} to 0.02 (center record). Increasing cytoplasmic [Mg^{2+}] to 300 μM further decreased P_{MCa} to 0.09 and P_{oB} to 0.00 (lower record). In this experiment, increasing cytoplasmic [Mg^{2+}] reduced P_{MCa} with $K_{0.5}$ = 30 ± 8 μM. Similar results were obtained with another low activity channel.

The moderate activity channel illustrated in Figure 7B displayed P_{MCa} = 0.95 and P_{oB} = 0.28 in 10 μM cytoplasmic [Ca^{2+}] plus 10 μM cytoplasmic [Mg^{2+}] and 5 nM MCa (top

record). Subsequent increase of cytoplasmic [Mg^{2+}] to 30 μM had negligible effect on both P_{MCa} and P_{oB} (center record), whereas further increase to 100 μM free [Mg^{2+}] decreased P_{MCa} to 0.24 and P_{oB} to 0.09 (lower record). In three independent experiments with moderate activity channels, cytoplasmic [Mg^{2+}] reduced P_{MCa} and P_{oB} with $K_{0.5}$ of 72 ± 19 μM and 61 ± 13 μM, respectively. Therefore, the apparent affinity values of cytoplasmic [Mg^{2+}] for inhibition of P_{MCa} and P_{oB} were comparable (p=0.662), favoring the possibility that both effects are related. Moreover, the apparent affinity of Mg^{2+} inhibitory effects is seemingly higher in low than in moderate activity RyR1 channels.

4. DISCUSSION

As pointed out earlier [26], Ca^{2+} release from the SR is significantly more sensitive to redox agents than Ca^{2+} uptake. The remarkable effects of redox agents on SR Ca^{2+} release reside in the great sensitivity of RyR1 channels to oxidizing/reducing agents, which by changing RyR1 redox state define the response of the channel to agonists and inhibitors. Several authors have proposed that RyR channels act as cellular redox sensors [26-29]. The redox state of a few highly reactive cysteine residues, defined as such because they react with redox agents at physiological pH, determines RyR channel activation/inhibition by physiological agonists/inhibitors, and in particular, it conditions how RyR channels respond to changes in cytoplasmic [Ca^{2+}] or [Mg^{2+}] [4].

The results presented in this work show that redox reagents modify the agonist effects of MCa on skeletal RyR1 in a complex manner. The sulfhydryl-reducing reagent DTT, which strongly inhibits RyR1 channel activation by Ca^{2+} [8], did not prevent the

stimulation of Ca^{2+} release, or the opening of RyR1 single channels to a sub-conductance state, produced by MCa addition at near resting [Ca^{2+}] levels (0.1 µM [Ca^{2+}]). Moreover, MCa increased [^{3}H]-ryanodine binding to DTT-treated vesicles two-fold when compared with native vesicles. In contrast, at 0.1 µM [Ca^{2+}] the oxidizing reagent thimerosal prevented both MCa-induced Ca^{2+} release from SR vesicles and the emergence of the typical sub-conductance state induced by MCa in single RyR1 channels. Thus, the present results concerning the effects of redox agents on the agonist action of MCa on Ca^{2+} efflux, ryanodine binding and single channel sub-conductance opening, provide a consistent framework.

The fact, however, that P_{MCa} decreased as single channel activity diminished when lowering cytoplasmic [Ca^{2+}] (Figs. 2-4), discards the possibility that the redox-sensitivity of the agonist effects of MCa is simply due to an increase in the apparent affinity of Ca^{2+} binding site(s) involved in RyR1 activation. If this were the case, an oxidizing agent such as thimerosal that favors channel activation by low [Ca^{2+}], should have increased P_{MCa}; likewise, moderate activity channels should have displayed more activation by MCa than low activity channels, exactly the opposite effects as those observed. Therefore, we propose that in spite of the inhibition of RyR1 channel activation by Ca^{2+} produced by reducing agents, the reduction of RyR1 cysteine residues enhances the binding affinity of MCa to RyR1. Accordingly, the stimulation by MCa of RyR1-mediated Ca^{2+} release at 0.1 µM [Ca^{2+}] under reducing conditions would arise from increased MCa binding to reduced RyR1 (or low activity) channels, which are poorly activated by low [Ca^{2+}] but would have high affinity for MCa binding. On the contrary, at resting [Ca^{2+}] oxidized RyR1 (or

moderate activity) channels would exhibit scant MCa binding in spite of their higher activity, due to their lower affinity for MCa.

The simplest way to explain how both low and moderate activity channels decreased P_{MCa} when channel activity diminished on lowering [Ca^{2+}] or increasing [Mg^{2+}] (see below) is to propose that the binding site(s) for MCa in RyR1 are freely accessible in the open channel state. This feature may explain why MCa does not elicit Ca^{2+} release when injected into resting skeletal muscle fibers [30], in which RyR1 channels are closed due to their mechanical interaction with the II-III loop of the neighboring DHPR [31-33]. A previous study suggested that MCa binds to RyR1 channels that open on membrane depolarization and that this interaction specifically alters the process of repolarization-induced closure of the channels [30]. Furthermore, voltage-activated low-amplitude local Ca^{2+} signals persist after fiber repolarization in the presence of MCa [34]. Based on these combined results, we propose that MCa binding to open RyR1 channels gives rise to the MCa-induced sub-conductance state that transiently keeps the channels refractory to DHPR-induced closing after repolarization.

Single channel experiments show that cytoplasmic [Mg^{2+}] reduced the agonist effect of MCa on RyR1. Since the apparent affinity of [Mg^{2+}] for the inhibitory effects on P_{MCa} and on P_{oB} were comparable, the most straightforward mechanism of inhibition of the agonist effect of MCa on RyR1 channel is the inhibition of P_o by Mg^{2+}, with no modification in RyR1 affinity for MCa binding. We report here that MCa induces a significant decrease in Mg^{2+} inhibition of [^{3}H]-ryanodine binding to native RyR1 channels, suggesting that MCa binding to the RyR1 protein produces a decrease in the Mg^{2+} affinity of its Ca^{2+}/Mg^{2+} inhibitory sites. Previous studies indicate that RyR1 oxidation also

decreases RyR1 sensitivity to Mg^{2+} inhibition [9, 11]. Moreover, reducing agents seem to increase markedly the affinity of RyR1 channels for MCa, suggesting the presence of cysteine residues in the MCa binding site(s). Maurocalcine binds to two discrete RyR1 regions, fragment 3 (residues 1021– 1631) and fragment 7 (residues 3201– 3661) [35]. Noteworthy, one cysteine residue susceptible to S-glutathionylation (Cys1591) is present in fragment 3 whereas fragment 7 contains a cysteine residue (Cys3635) that is susceptible to S-glutathionylation, S-nitrosylation and disulfide oxidation [6]. In addition, another cysteine residue (Cys3193) susceptible to S-glutathionylation is situated only eight amino acids away from the beginning of fragment 7. Based on the present results, we suggest that MCa binding to RyR1 modifies the environment of one or more of these cysteine residues, resulting in a decreased affinity for Mg^{2+}. Conversely, modification of these residues by oxidation with thimerosal would decrease the affinity of MCa binding to RyR1, albeit we cannot rule out other possibilities. Accordingly, it would be of interest to study if mutations of these three particular cysteine residues affect the stimulation of RyR1 activity by MCa.

ACKNOWLEDGMENTS

This work was supported by FONDECYT-FONDAP 15010006, ECOS-CONICYT C05B03 and ECOS-SUD. Hicham Bichraoui was a recipient from the Association Francaise contre les Myopathies.

ABREVIATIONS

$[Ca^{2+}]$	=	free calcium concentration
$[Mg^{2+}]$	=	free magnesium concentration
DHPR	=	dihydropyridine receptor
DTT	=	dithiothreitol
EGTA	=	ethyleneglycol-bis(ß-aminoethyl ether) N, N, N', N'-tetraacetic acid
HEDTA	=	N-(2-hydroxyethyl)-ethylenediamine-triacetic acid
MCa	=	Maurocalcine
P_{MCa}	=	fractional time spent by the channel in the sub-conductance state induced by Maurocalcine
P_o	=	fractional time spent by the channel in the open state
P_{oB}	=	fractional time spent by the channel in the open state, excluding the time spent in the sub-conductance state induced by Maurocalcine
RyR	=	Ryanodine receptor
RyR1	=	type-1 Ryanodine receptor
SE	=	standard error
SERCA	=	sarcoplamic/endoplasmic Ca^{2+}-ATPase
SR	=	sarcoplasmic reticulum

REFERENCES

1. M. Fill, J.A. Copello, Ryanodine receptor calcium release channels, Physiol Rev. 82 (2002) 893-922.

2. E. Rios, G. Brum, Involvement of dihydropyridine receptors in excitation-contraction coupling in skeletal muscle, Nature. 325 (1987) 717-720.

3. R. Bull, J.P. Finkelstein, A. Humeres, M.I. Behrens, C. Hidalgo, Effects of ATP, Mg^{2+}, and redox agents on the Ca^{2+} dependence of RyR channels from rat brain cortex, Am J Physiol Cell Physiol. 293 (2007) C162-171.

4. C. Hidalgo, P. Donoso, Crosstalk between calcium and redox signaling: from molecular mechanisms to health implications, Antioxid Redox Signal. 10 (2008) 1275-1312.

5. A.A. Voss, J. Lango, M. Ernst-Russell, D. Morin, I.N. Pessah, Identification of hyperreactive cysteines within ryanodine receptor type 1 by mass spectrometry, J Biol Chem. 279 (2004) 34514-34520.

6. P. Aracena-Parks, S.A. Goonasekera, C.P. Gilman, R.T. Dirksen, C. Hidalgo, S.L. Hamilton, Identification of cysteines involved in S-nitrosylation, S-glutathionylation, and oxidation to disulfides in ryanodine receptor type 1, J Biol Chem. 281 (2006) 40354-40368.

7. J. Suko, G. Hellmann, Modification of sulfhydryls of the skeletal muscle calcium release channel by organic mercurial compounds alters Ca^{2+} affinity of regulatory Ca^{2+} sites in single channel recordings and [^{3}H]ryanodine binding, Biochim Biophys Acta. 1404 (1998) 435-450.

8. J.J. Marengo, C. Hidalgo, R. Bull, Sulfhydryl oxidation modifies the calcium dependence of ryanodine-sensitive calcium channels of excitable cells, Biophys J. 74 (1998) 1263-1277.

9. P. Donoso, P. Aracena, C. Hidalgo, Sulfhydryl oxidation overrides Mg^{2+} inhibition of calcium-induced calcium release in skeletal muscle triads, Biophys J. 79 (2000) 279-286.

10. J. Suko, G. Hellmann, H. Drobny, Modulation of the calmodulin-induced inhibition of sarcoplasmic reticulum calcium release channel (ryanodine receptor) by sulfhydryl oxidation in single channel current recordings and [(3)H]ryanodine binding, J Membr Biol. 174 (2000) 105-120.

11. P. Aracena, G. Sanchez, P. Donoso, S.L. Hamilton, C. Hidalgo, S-glutathionylation decreases Mg^{2+} inhibition and S-nitrosylation enhances Ca^{2+} activation of RyR1 channels, J Biol Chem. 278 (2003) 42927-42935.

12. H. Westerblad, D.G. Allen, Emerging roles of ROS/RNS in muscle function and fatigue, Antioxid Redox Signal. 15 (2011) 2487-2499.

13. A. Mosbah, R. Kharrat, Z. Fajloun, J.G. Renisio, E. Blanc, J.M. Sabatier, M. El Ayeb, H. Darbon, A new fold in the scorpion toxin family, associated with an activity on a ryanodine-sensitive calcium channel, Proteins. 40 (2000) 436-442.

14. E. Esteve, K. Mabrouk, A. Dupuis, S. Smida-Rezgui, X. Altafaj, D. Grunwald, J.C. Platel, N. Andreotti, I. Marty, J.M. Sabatier, M. Ronjat, M. De Waard, Transduction of the scorpion toxin maurocalcine into cells. Evidence that the toxin crosses the plasma membrane, J Biol Chem. 280 (2005) 12833-12839.

15. Z. Fajloun, R. Kharrat, L. Chen, C. Lecomte, E. Di Luccio, D. Bichet, M. El Ayeb, H. Rochat, P.D. Allen, I.N. Pessah, M. De Waard, J.M. Sabatier, Chemical synthesis and characterization of maurocalcine, a scorpion toxin that activates Ca^{2+} release channel/ryanodine receptors, FEBS Lett. 469 (2000) 179-185.

16. L. Chen, E. Esteve, J.M. Sabatier, M. Ronjat, M. De Waard, P.D. Allen, I.N. Pessah, Maurocalcine and peptide A stabilize distinct subconductance states of ryanodine receptor type 1, revealing a proportional gating mechanism, J Biol Chem. 278 (2003) 16095-16106.

17. E. Esteve, S. Smida-Rezgui, S. Sarkozi, C. Szegedi, I. Regaya, L. Chen, X. Altafaj, H. Rochat, P. Allen, I.N. Pessah, I. Marty, J.M. Sabatier, I. Jona, M. De Waard, M. Ronjat, Critical amino acid residues determine the binding affinity and the Ca^{2+} release efficacy of maurocalcine in skeletal muscle cells, J Biol Chem. 278 (2003) 37822-37831.

18. C. Hidalgo, J. Jorquera, V. Tapia, P. Donoso, Triads and transverse tubules isolated from skeletal muscle contain high levels of inositol 1,4,5-trisphosphate, J Biol Chem. 268 (1993) 15111-15117.

19. R. Bull, J.J. Marengo, B.A. Suarez-Isla, P. Donoso, J.L. Sutko, C. Hidalgo, Activation of calcium channels in sarcoplasmic reticulum from frog muscle by nanomolar concentrations of ryanodine, Biophys J. 56 (1989) 749-756.

20. R. Bull, J.J. Marengo, Sarcoplasmic reticulum release channels from frog skeletal muscle display two types of calcium dependence, FEBS Lett. 331 (1993) 223-227.

21. J.J. Marengo, R. Bull, C. Hidalgo, Calcium dependence of ryanodine-sensitive calcium channels from brain cortex endoplasmic reticulum, FEBS Lett. 383 (1996) 59-62.

22. R. Bull, J.J. Marengo, J.P. Finkelstein, M.I. Behrens, O. Alvarez, SH oxidation coordinates subunits of rat brain ryanodine receptor channels activated by calcium and ATP, Am J Physiol Cell Physiol. 285 (2003) C119-128.

23. R. Coronado, J. Morrissette, M. Sukhareva, D.M. Vaughan, Structure and function of ryanodine receptors, Am J Physiol. 266 (1994) C1485-1504.

24. G. Meissner, Ryanodine receptor/Ca^{2+} release channels and their regulation by endogenous effectors, Annu Rev Physiol. 56 (1994) 485-508.

25. M. Fill, R. Coronado, J.R. Mickelson, J. Vilven, J.J. Ma, B.A. Jacobson, C.F. Louis, Abnormal ryanodine receptor channels in malignant hyperthermia, Biophys J. 57 (1990) 471-475.

26. I.N. Pessah, K.H. Kim, W. Feng, Redox sensing properties of the ryanodine receptor complex, Front Biosci. 7 (2002) a72-79.

27. J.P. Eu, J. Sun, L. Xu, J.S. Stamler, G. Meissner, The skeletal muscle calcium release channel: coupled O2 sensor and NO signaling functions, Cell. 102 (2000) 499-509.

28. R. Xia, T. Stangler, J.J. Abramson, Skeletal muscle ryanodine receptor is a redox sensor with a well defined redox potential that is sensitive to channel modulators, J Biol Chem. 275 (2000) 36556-36561.

29. C. Hidalgo, Cross talk between Ca^{2+} and redox signalling cascades in muscle and neurons through the combined activation of ryanodine receptors/Ca^{2+} release channels, Philos Trans R Soc Lond B Biol Sci. 360 (2005) 2237-2246.

30. S. Pouvreau, L. Csernoch, B. Allard, J.M. Sabatier, M. De Waard, M. Ronjat, V. Jacquemond, Transient loss of voltage control of Ca^{2+} release in the presence of maurocalcine in skeletal muscle, Biophys J. 91 (2006) 2206-2215.

31. T. Tanabe, K.G. Beam, B.A. Adams, T. Niidome, S. Numa, Regions of the skeletal muscle dihydropyridine receptor critical for excitation-contraction coupling, Nature. 346 (1990) 567-569.

32. X. Lu, L. Xu, G. Meissner, Activation of the skeletal muscle calcium release channel by a cytoplasmic loop of the dihydropyridine receptor, J Biol Chem. 269 (1994) 6511-6516.

33. J. Nakai, T. Tanabe, T. Konno, B. Adams, K.G. Beam, Localization in the II-III loop of the dihydropyridine receptor of a sequence critical for excitation-contraction coupling, J Biol Chem. 273 (1998) 24983-24986.

34. L. Csernoch, S. Pouvreau, M. Ronjat, V. Jacquemond, Voltage-activated elementary calcium release events in isolated mouse skeletal muscle fibers. J Membr Biol. 226 (2008) 43-55.

35. X. Altafaj, W. Cheng, E. Esteve, J. Urbani, D. Grunwald, J.M. Sabatier, R. Coronado, M. De Waard, M. Ronjat, Maurocalcine and domain A of the II-III loop of the dihydropyridine receptor Cav 1.1 subunit share common binding sites on the skeletal ryanodine receptor, J Biol Chem. 280 (2005) 4013-4016.

FIGURE LEGENDS

Figure 1. Effects of MCa on Ca^{2+} release from actively loaded triad-enriched SR vesicles. Active loading with Ca^{2+} was initiated by addition of ATP-Mg, as indicated in the figure. Changes in extravesicular [Ca^{2+}] were determined with Calcium Green-2, as detailed in Materials and Methods. In the three representative experiments illustrated (Panels A-C), addition of ATP-Mg promoted fast Ca^{2+} uptake, and decreased probe fluorescence to a steady value corresponding to an extravesicular [Ca^{2+}] < 150 nM (see Results). Subsequent addition of MCa caused effective and transient Ca^{2+} release from native vesicles (Panel A) or from vesicles pre-incubated for 30 min with 10 mM DTT (Panel B). Addition of the sulfhydryl oxidizing agent thimerosal after completion of Ca^{2+} uptake prevented Ca^{2+} release induced by MCa but not by caffeine (Panel C).

Figure 2. Maurocalcine enhances [^{3}H] ryanodine binding to triad-enriched SR vesicles and decreases the inhibitory effects of Mg^{2+}. As illustrated in **Panel A**, incubation of native vesicles with 50 nM MCa stimulated equilibrium [^{3}H]-ryanodine binding density (light grey bar) relative to the values determined in the absence of MCa (empty bar). Vesicles incubated with DTT displayed lower [^{3}H]-ryanodine binding relative to native vesicles (Panel A, black bar). Addition of 50 nM MCa to DTT-treated SR vesicles increased [^{3}H]-ryanodine binding relative to vesicles incubated only with DTT (Panel A, dark grey bar). ***: $p < 0.0001$ calculated by One-way ANOVA followed by Dunnett's multiple comparison test. As illustrated in **Panel B**, incubation of native skeletal SR vesicles with 200 nM MCa significantly decreased the inhibitory effects of Mg^{2+} on

equilibrium [^{3}H]-ryanodine binding. Fitting the experimental points to a non-linear Hill function yielded n_{Hill} =1.0 ± 0.1 and K_i = 125.3 ± 8.8 μM for native vesicles, and n_{Hill} = 1.4 ± 0.1 and K_i = 676.4 ± 49.0 μM for native SR vesicles incubated with 200 nM MCa.Values represent Mean ± SE (N=3).

Figure 3. Effects of MCa on a low activity RyR1 channel. Representative current recordings obtained with the same low activity single RyR1 channel in the absence (Panel A) or at 5 nM MCa (Panel B). P_{MCa} and P_{oB} values, calculated for the whole recorded periods (at least 180 s) and the free cytoplasmic [Ca^{2+}] are depicted above each current trace. Addition of MCa induced channel openings to a well-defined sub-conductance current level, indicated by an arrow at the right of the current traces. Sequential reduction of cytoplasmic [Ca^{2+}] using HEDTA and/or EGTA (see Materials and Methods), progressively reduced both P_{MCa} and P_{oB} (second and third trace).

Figure 4. Effects of MCa on a moderate activity RyR1 channel. Representative current recordings of the same moderate activity single RyR1 channel obtained in the absence (Panel A) or at 5 nM MCa (Panel B). P_{MCa} and P_{oB} values, calculated for the whole recorded periods (at least 150 s) and the free cytoplasmic [Ca^{2+}] are depicted above each current trace. Addition of MCa prompted the emergence of the sub-conductance current level, as indicated by an arrow at the right of the top and middle traces of Panel B. Sequential reduction of cytoplasmic [Ca^{2+}] using HEDTA and/or EGTA (see Materials and Methods), progressively reduced both P_{MCa} and P_{oB} (second and third trace). Notice that P_{MCa} and P_{oB} values were equal to 0.00 at 0.1 μM [Ca^{2+}].

Figure 5. Comparative effects of MCa on low and moderate activity RyR1 channels. Bars represent mean P_o, P_{oB} and P_{MCa} values (± SE) obtained from several single channels that spontaneously displayed either low (empty bars) or moderate activity (black bars). As illustrated in **Panel A**, addition of 5 nM MCa at 10 µM [Ca^{2+}] induced the sub-conductance state in both low and moderate activity channels. In contrast, as illustrated in **Panel B**, addition of 5 nM MCa at 0.1 µM [Ca^{2+}] modified only low activity channels. Numbers above or on each bar represent the number of single channel data included in each condition. *: $p < 0.05$; **: $p = 0.001$.

Figure 6. Thimerosal treatment inhibited MCa activation of a single RyR1 channel at 0.1 µM [Ca^{2+}]. **Panel A** shows representative current recordings obtained from a single low activity channel at the indicated cytoplasmic [Ca^{2+}] before (upper trace) and after addition of MCa (lower trace). Sub-conductance current level is indicated, as usual, with an arrow at the right of lower trace. P_{MCa} and P_{oB} values, calculated for the whole recorded periods (at least 70 s) and cytoplasmic [Ca^{2+}] are displayed above each trace. **Panel B** was obtained with the same channel recorded in Panel A, after incubation with 200 µM thimerosal for 80 s followed by extensive perfusion of the cis chamber to eliminate non reacted thimerosal (for further details, see Results). At 0.1 µM [Ca^{2+}], addition of 5 nM MCa did not elicit the sub-conductance state displayed by the channel before incubation with thimerosal (compare trace in Panel B with lower trace in Panel A).

Figure 7. Mg^{2+} inhibits the effects of Maurocalcine on low and moderate activity RyR1 channels. Representative current recordings were obtained, at 10 µM cytoplasmic [Ca^{2+}] and in the presence of 5 nM MCa, from single channels that spontaneously displayed either low (**Panel A**) or moderate activity (**Panel B**). In each case, the same channel was sequentially exposed to increasing cytoplasmic [Mg^{2+}], as indicated near each current trace. P_{MCa} and P_{oB} values, calculated from the whole recorded periods (at least 180 s), are depicted above the recordings. The arrows indicate the sub-conductance current level induced by MCa.

Figure 1

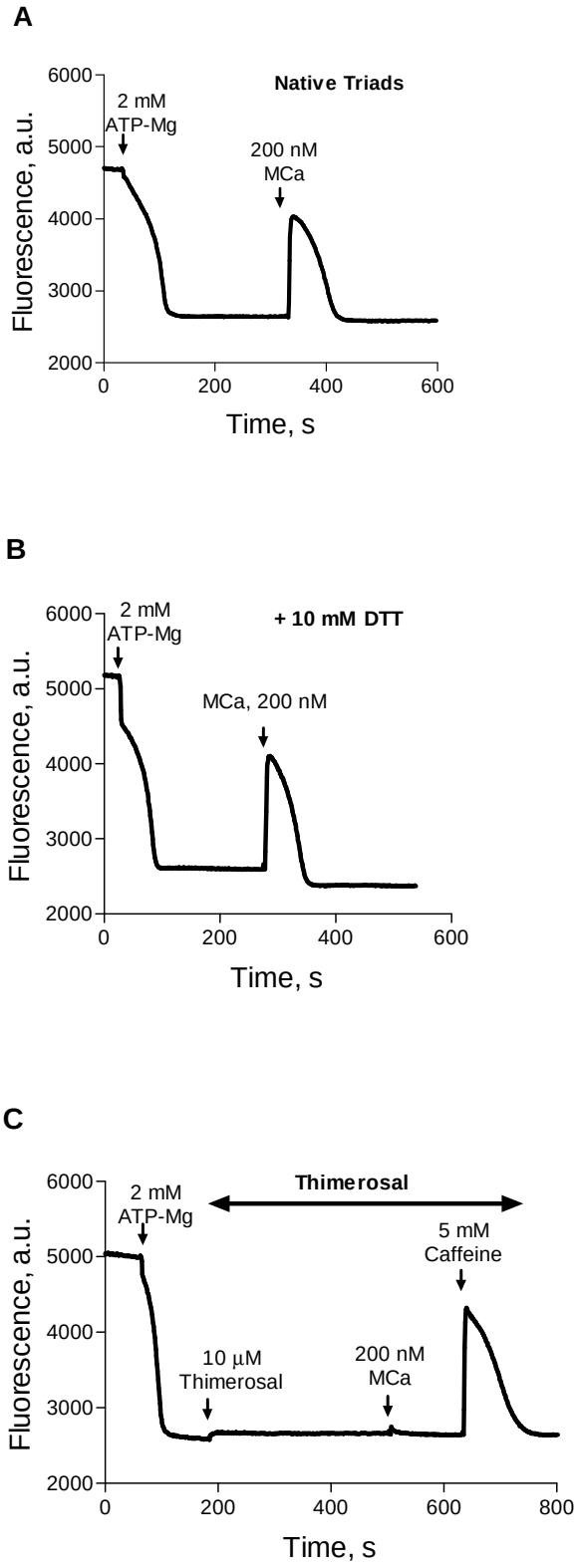
A
Native Triads
2 mM
ATP-Mg
200 nM
MCa
Fluorescence, a.u.
Time, s
B
2 mM
ATP-Mg
+ 10 mM DTT
MCa, 200 nM
Fluorescence, a.u.
Time, s
C
Thimerosal
2 mM
ATP-Mg
5 mM
Caffeine
10 µM
Thimerosal
200 nM
MCa
Fluorescence, a.u.
Time, s

Figure 2

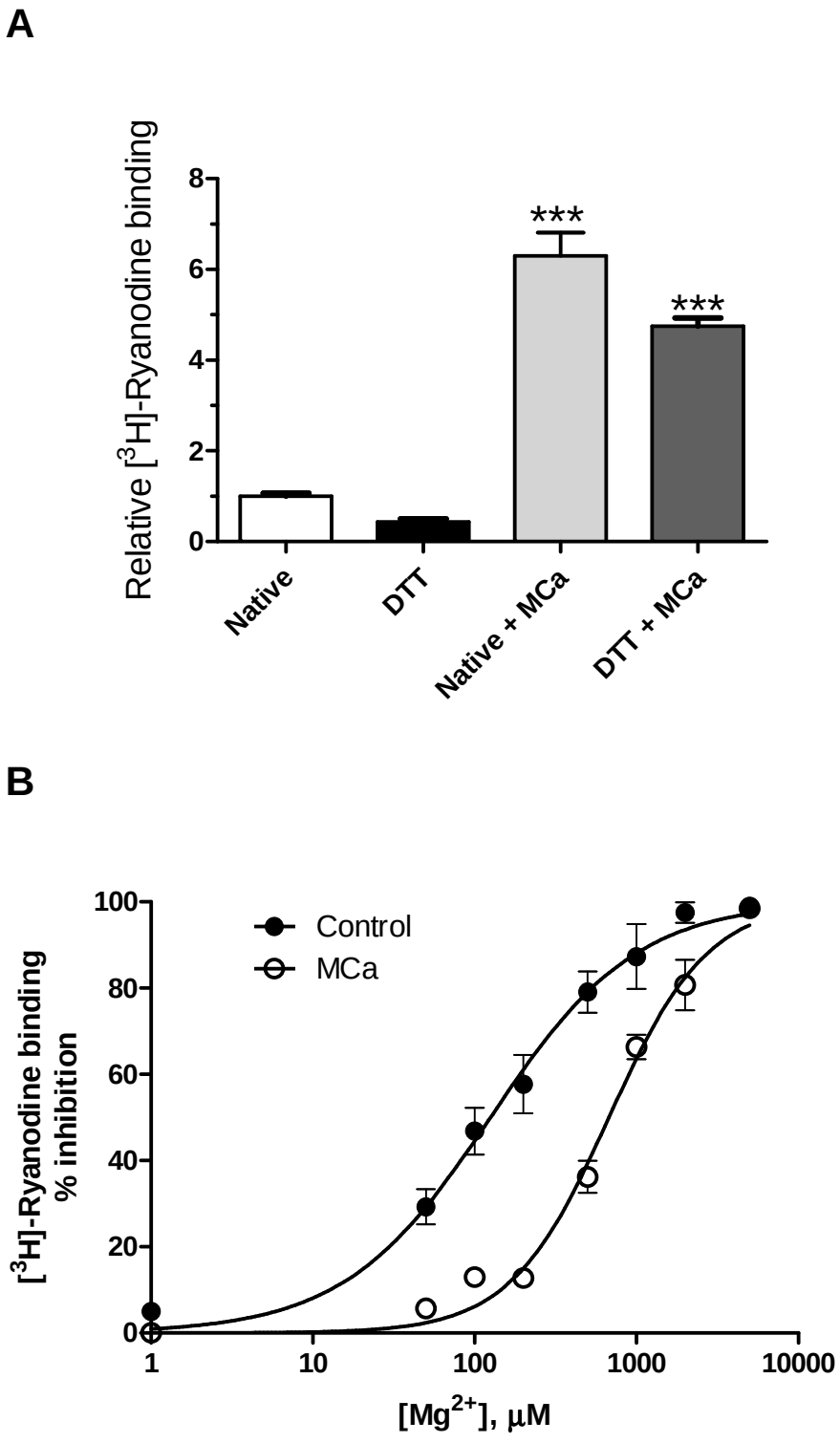
A
Relative [3H]-Ryanodine binding
8
6
4
2
0
***
***
Native
DTT
Native + MCa
DTT + MCa
B
[3H]-Ryanodine binding
% inhibition
100
80
60
40
20
0
Control
MCa
1
10
100
1000
10000
[Mg2+], µM

Figure 3

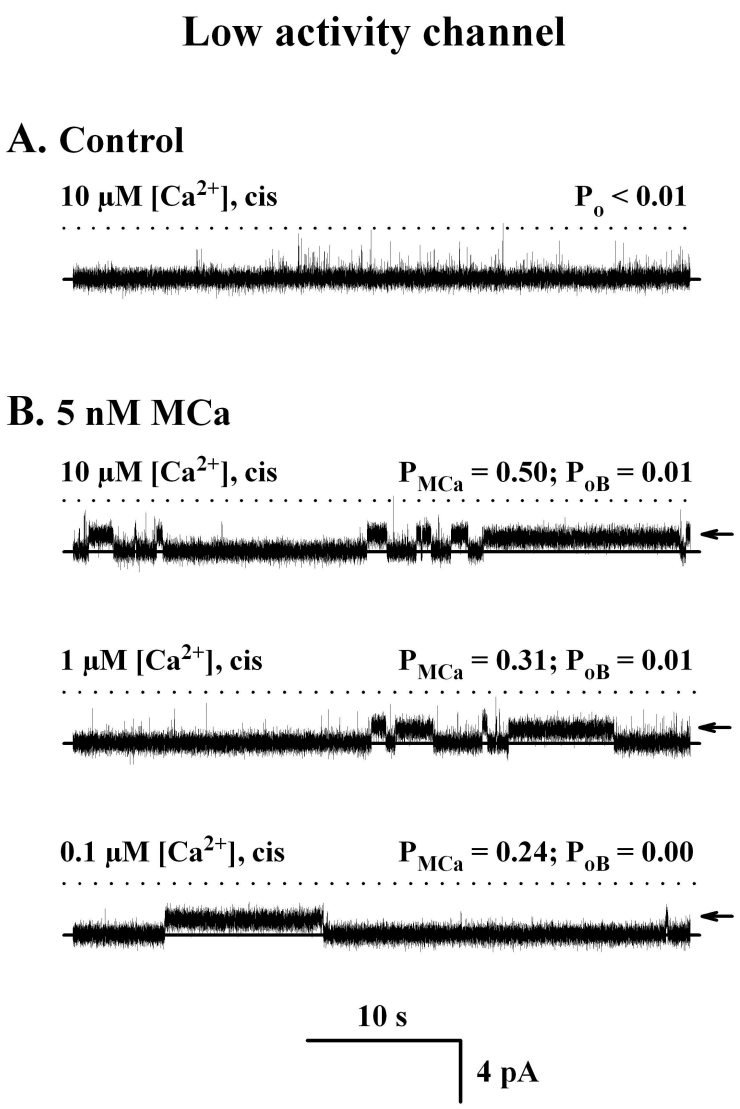
Low activity channel
A. Control
10 µM [Ca2+], cis
Po < 0.01
B. 5 nM MCa
10 µM [Ca2+], cis
PMCa = 0.50; PoB = 0.01
1 µM [Ca2+], cis
PMCa = 0.31; PoB = 0.01
0.1 µM [Ca2+], cis
PMCa = 0.24; PoB = 0.00
10 s
4 pA

Figure 4

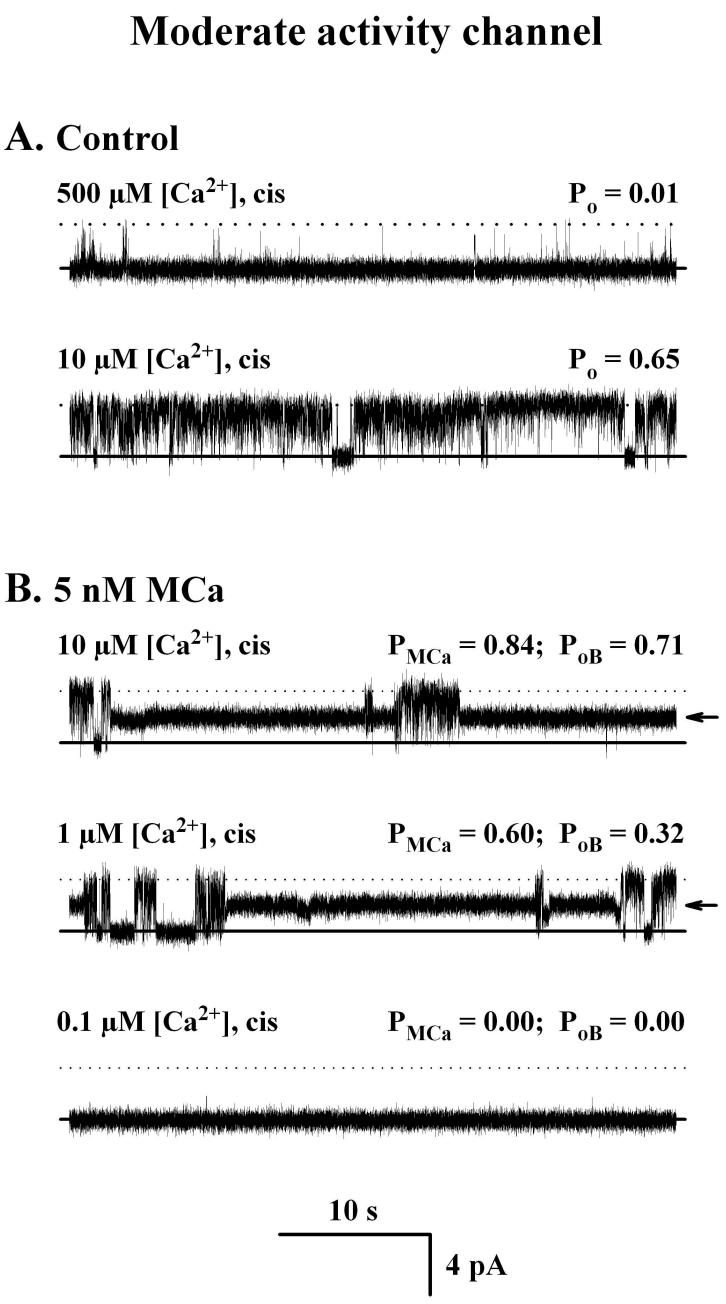
Moderate activity channel
A. Control
500 µM [Ca2+], cis
Po = 0.01
10 µM [Ca2+], cis
Po = 0.65
B. 5 nM MCa
10 µM [Ca2+], cis
PMCa = 0.84; PoB = 0.71
1 µM [Ca2+], cis
PMCa = 0.60; PoB = 0.32
0.1 µM [Ca2+], cis
PMCa = 0.00; PoB = 0.00
10 s
4 pA

Figure 5

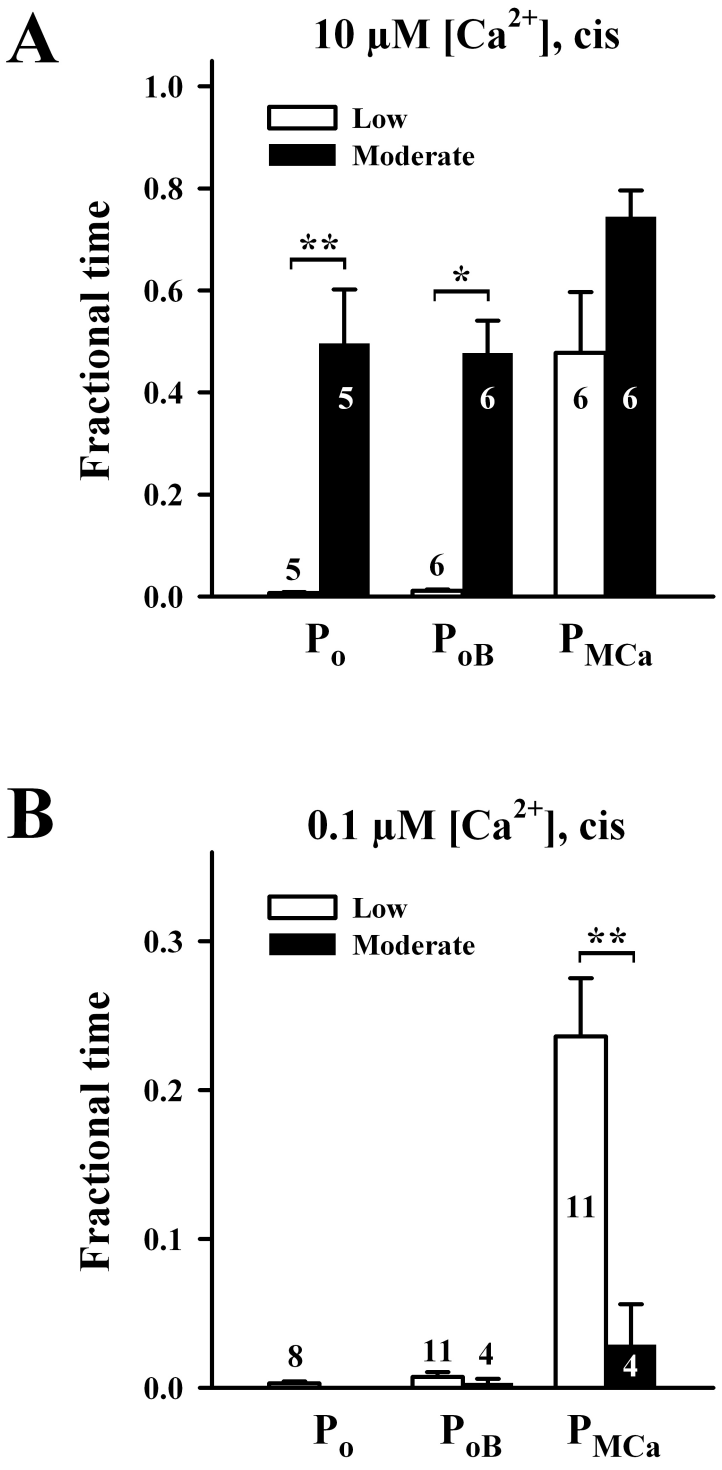
A
10 µM [Ca2+], cis
Low
Moderate
Fractional time
1.0
0.8
0.6
0.4
0.2
0.0
**
*
5
6
6
6
5
6
Po
PoB
PMCa
B
0.1 µM [Ca2+], cis
Low
Moderate
Fractional time
0.3
0.2
0.1
0.0
**
11
8
11
4
4
Po
PoB
PMCa

Figure 6

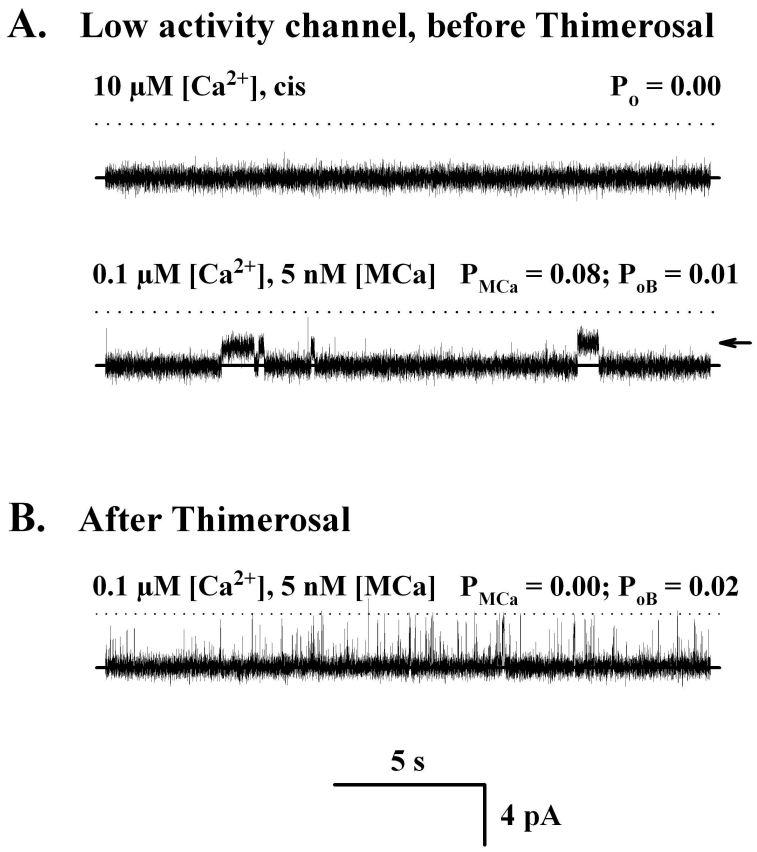
A. Low activity channel, before Thimerosal
10 µM [Ca2+], cis
Po = 0.00
0.1 µM [Ca2+], 5 nM [MCa]
PMCa = 0.08; PoB = 0.01
B. After Thimerosal
0.1 µM [Ca2+], 5 nM [MCa]
PMCa = 0.00; PoB = 0.02
5 s
4 pA

Figure 7

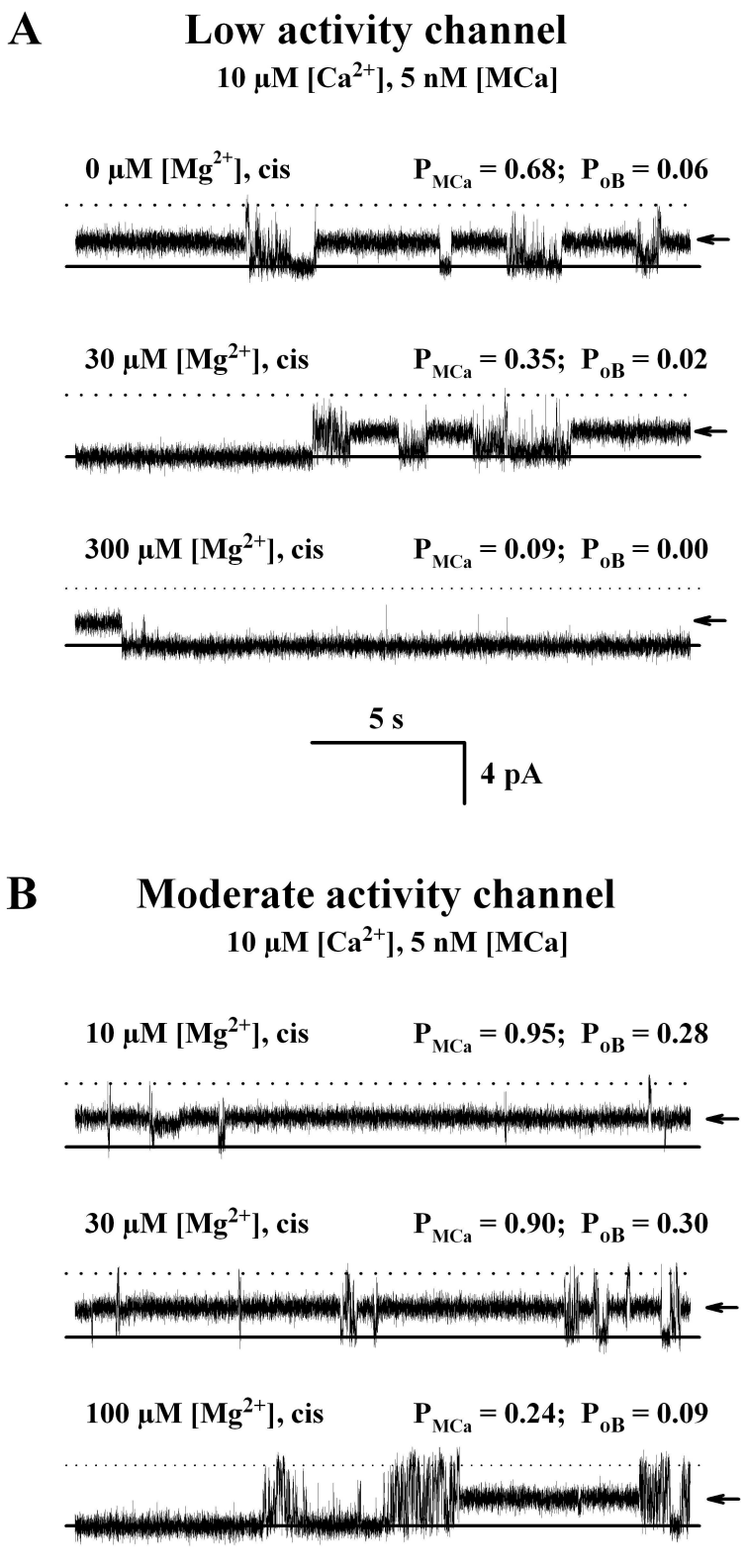
A
Low activity channel
10 µM [Ca2+], 5 nM [MCa]
0 µM [Mg2+], cis
PMCa = 0.68; PoB = 0.06
30 µM [Mg2+], cis
PMCa = 0.35; PoB = 0.02
300 µM [Mg2+], cis
PMCa = 0.09; PoB = 0.00
5 s
4 pA
B
Moderate activity channel
10 µM [Ca2+], 5 nM [MCa]
10 µM [Mg2+], cis
PMCa = 0.95; PoB = 0.28
30 µM [Mg2+], cis
PMCa = 0.90; PoB = 0.30
100 µM [Mg2+], cis
PMCa = 0.24; PoB = 0.09

SUPPLEMENTARY MATERIAL

Figure legends

Figure S1. Graphical representation of P_{MCa} and P_{oB}. To calculate P_{MCa} values we added all individual dwell times in which the channel spent in the MCa-induced sub-conductance state, defined as s_i, and divided this sum by the total recorded time. To calculate P_{oB} values we added all o_j values, which represent the channel dwell time in the full open state, and divided this sum by the sum of the b_i values, which represent the dwell times in which the channel did not reside in the MCa-induced sub-conductance state.

Figure S2. Single RyR1 channels spontaneously display three different responses to cytoplasmic [Ca^{2+}]. These responses include the ***low activity*** response (filled triangles), characterized by P_o values < 0.1 in the [Ca^{2+}] range 0.1-500 μM; the ***moderate activity*** response (open circles) with maximal P_o in the 10-30 μM [Ca^{2+}] range and P_o < 0.1 at 0.1 or 500 μM [Ca^{2+}], and the ***high activity*** response (filled circles) characterized by significant activity at 0.1 μM [Ca^{2+}] and P_o close to 1.0 in the 1.0-500 μM [Ca^{2+}] range. The **low activity** response data are displayed in an expanded vertical scale in the inset.